Far-infrared and near-millimetre dielectric response of DRADP-50 dipolar glass compared with that of RADP

1993 J. Phys.: Condens. Matter 5 3573

(http://iopscience.iop.org/0953-8984/5/22/009)

J. Phys.: Condens. Matter 5 (1993) 3573–3586. Printed in the UK

Far-infrared and near-millimetre dielectric response of DRADP-50 dipolar glass compared with that of RADP

J Petzelt†, S Kamba†, A V Sinitski‡, A G Pimenov‡, A A Volkov‡, G V Kozlov‡ and R Kind§

† Institute of Physics, Czech Academy of Sciences, 180 40 Prague 8, Czech Republic
‡ Institute of General Physics, Russian Academy of Sciences, 117 942 Moscow, Russia
§ Institute of Quantum Electronics, ETH Hönggerberg, CH-8093 Zurich, Switzerland

Received 15 December 1992

Abstract. The far-infrared and near-millimetre dielectric response of $Rb_{0.5}(ND_4)_{0.5}D_2PO_4$ (DRADP) has been determined by evaluation of reflectivity (15–650 cm^{-1}) and complex transmittance (5–18 cm^{-1}) spectra at temperatures of 10–300 K. Comparison with the response of $Rb_{0.5}(NH_4)_{0.5}H_2PO_4$ (RADP) shows a very pronounced isotopic effect and strong coupling of the proton motion to several polar phonon modes apparently reduced in the case of deuterium. Also the broad background absorption observed previously in RADP is absent in DRADP, which suggests an important role of quantum tunnelling in the former case. The loss maxima due to acid deuteron hopping (including lower-frequency data from He) in the broad temperature range 300–60 K can be well fitted with the Vogel–Fulcher dependence ($T_{VF} \simeq 34$ K, $E_0 = 410$ K, $\nu_\infty = 1.2 \times 10^{12}$ Hz). However, in agreement with several other experiments, above ~ 120 K the deuteron mode is monodispersive and the Debye relaxation frequency within the accuracy limits also obeys the Arrhenius law ($E_0 = 500$ K, $\nu_\infty = 1.2 \times 10^{12}$ Hz).

1. Introduction

Mixed crystals of $Rb_{1-x}(NH_4)_xH_2PO_4$ (RADP) and $Rb_{1-x}(ND_4)_xD_2PO_4$ (DRADP) form dipolar glasses for $0.3 \leqslant x \leqslant 0.7$, which belong to the best-investigated glass systems of all (Höchli *et al* 1990, Courtens 1987). In the previous paper (Petzelt *et al* 1991) we presented far-infrared (FIR) and near-millimetre dielectric data (2×10^{11} to 2×10^{13} Hz) on a protonated system for $x = 0.5$ (RADP-50). The essential result was that at high temperatures $T \geqslant 100$ K a simple relaxation soft-mode behaviour was observed with partial softening corresponding to a crystal with averaged structure. At lower temperatures further softening occurred accompanied by a strong decrease in the relaxation strength. According to lower-frequency dielectric data covering the broad range 10^2–10^{10} Hz (Courtens 1984, 1986, Brückner *et al* 1988, He *et al* 1990, He 1991) the soft mode goes over into a broad dielectric dispersion whose characteristic frequency ν_R obeys the Vogel–Fulcher law

$$\nu_R = \nu_\infty \exp[-E_0/(T - T_{VF})] \tag{1}$$

with $T_{VF} = 10$ K.

DRADP systems have been studied more intensively in recent years because deuteron dynamics is theoretically simpler (quantum tunnelling can be neglected down to low temperatures); also the deuterated systems are much more suitable for neutron scattering (Grimm 1989) and more convenient for nuclear magnetic resonance (NMR) investigations:

0953-8984/93/223573+14$07.50

deuteron and Rb NMR measurements made it possible to determine the Edwards–Anderson order parameter (Blinc *et al* 1989) and the local dynamic behaviour of deuterons (Blinc *et al* 1986a, b) and to distinguish between para-, ferro- and antiferroelectric and glass-type order (Kind *et al* 1990).

From the point of view of dielectric spectroscopy, deuterated glasses are also more convenient because the spectral loss peak due to deuteron hopping has lower frequency; it is sharper than in protonated glasses and well separated from higher-frequency absorption mechanisms (Courtens 1986, He *et al* 1990, He 1991). Similarly, in analogy to pure KH_2PO_4 (KDP)-like crystals, the high-temperature soft mode is also expected to lie well below all phonon frequencies (Simon 1992), so it can be better studied. From the point of view of infrared (IR) spectroscopy, comparison of deuterated and protonated samples may also give interesting information on the polar phonon eigenvectors and the role of protons (deuterons) in them.

In this paper we present the results of our FIR and near-millimetre dielectric measurements on DRADP-50 and try to connect them with the recently published lower-frequency dielectric data (He 1991). Special care will be devoted to a comparison of deuterated and protonated systems. Preliminary results of these measurements have already been published (Kamba *et al* 1992).

2. Experimental details

Single crystals of RADP-50 grown from a heavy-water solution (Arend *et al* 1986) have been cut and polished to obtain thick (0 0 1) and (1 0 0) plates ($d \simeq 2$ mm) for reflectivity measurements and thinner plane-parallel plates ($d \simeq 0.1$–0.5 mm) for transmission measurements (area about 0.3 cm^2). The degree of deuteration was estimated to be 99%.

Polarized reflectivity spectra in the 20–650 cm^{-1} range were measured at temperatures of 15–300 K using a Bruker IFS 113v Fourier interferometer. Power transmission measurements were carried out in the 15–100 cm^{-1} range with the same spectrometer using a liquid-helium-cooled germanium bolometer as a detector. Complex transmittance measurements (power transmission and phase of the transmitted light) in the 5–18 cm^{-1} range were performed with the home-made spectrometer Epsilon based on tunable backward-wave-oscillator sources (Volkov *et al* 1985).

In the case of reflectivity measurements we discovered striking differences between the fresh and old polished samples obviously caused by exchange of deuterium with hydrogen from the water vapour of the air (Kamba *et al* 1992). A similar effect is known to take place also in the case of KD_2PO_4 (DKDP) (Bréhat and Wyncke 1988). Therefore all the results presented here were obtained on surfaces freshly polished prior to our measurements.

3. Results and evaluation

Figures 1(*a*) and (*b*) show the temperature dependences of the reflectivity spectra of DRADP for the electric field polarizations $E \parallel c$ (B_2 modes) and $E \perp c$ (E modes) on a logarithmic frequency scale to expand the low-frequency part. The reflectivity calculated from the near-millimetre complex transmittance data is added at the low-frequency end. The whole reflectivity spectra were normalized in order to match the more accurate near-millimetre data.

The spectra were fitted with a model of classical damped oscillators describing the main observed polar phonons. A low-frequency Debye relaxation was added to fit the soft-mode

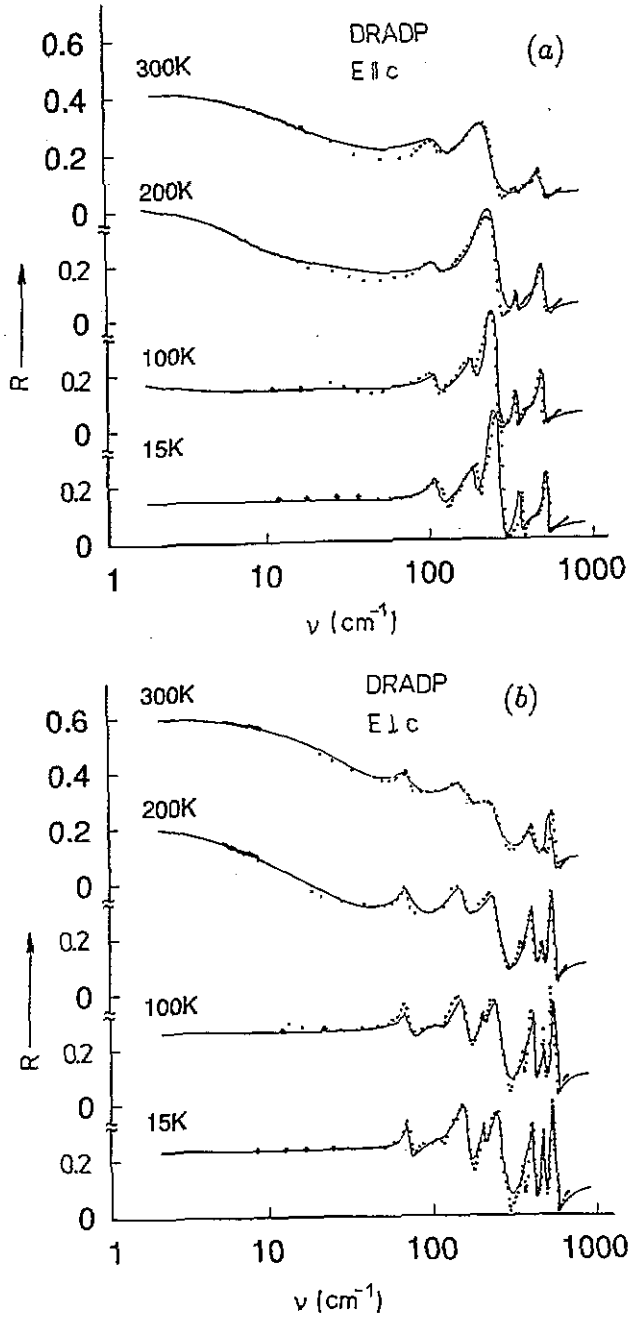

Figure 1. FIR reflectivity spectra of DRADP-50. Dots show experimental data; the full curve is the fit (see text). Dense dots in the near-millimetre range were calculated from complex transmittance data. Crosses in the submillimetre range at low temperatures were calculated from interference pattern in the transmission spectra. (*a*) $E \parallel c$ polarization, (*b*) $E \perp c$ polarization.

region. Five and nine oscillators were used to fit the spectra for the $E \parallel c$ and $E \perp c$ polarizations, respectively. The fitted curves are also shown in figure 1. In figures 2(*a*)

and (*b*) we show the near-millimetre $\epsilon'(\nu)$ and $\epsilon''(\nu)$ spectra (for selected temperatures) to which the relaxation parameters from the reflectivity fit were finally adjusted. The complete dielectric spectra from the fit in the 1–1000 cm^{-1} range with the power transmission data added are shown in figures 3(*a*) and (*b*).

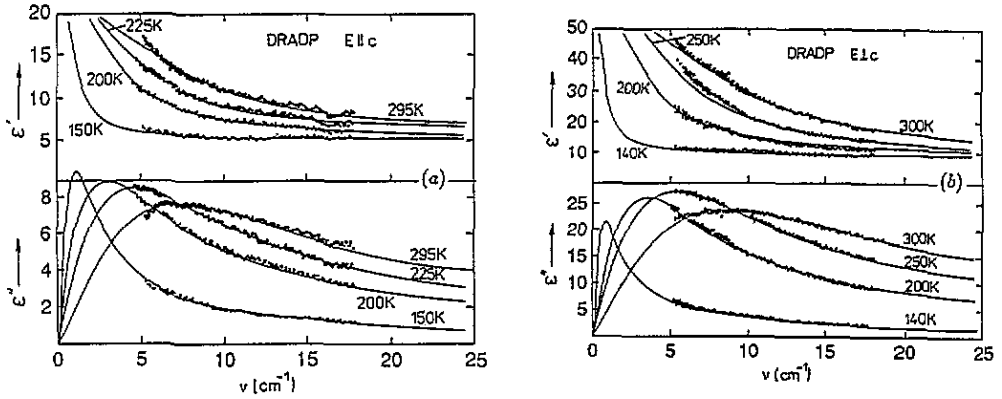

Figure 2. Dielectric spectra of DRADP calculated from the complex transmittance measurements with backward-wave-oscillator source. Dots—experiment; full curve—fit (see text). (*a*) $E \parallel c$ polarization, (*b*) $E \perp c$ polarization.

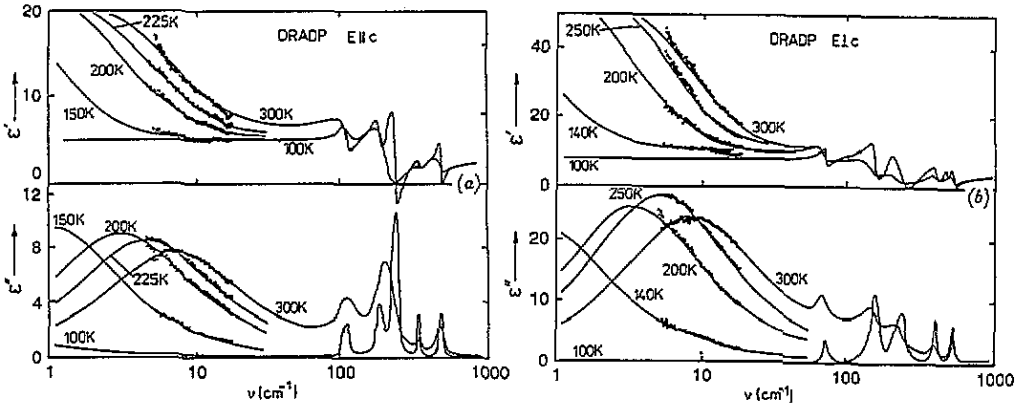

Figure 3. Dielectric spectra of DRADP in a broad spectral range. Dots—complex transmittance measurements; full curve—fit of complete measured spectra. (*a*) $E \parallel c$ polarization, (*b*) $E \perp c$ polarization.

4. Discussion

To facilitate the discussion, let us first compare our results on DRADP with those on RADP (Petzelt *et al* 1991). In figures 4(*a*) and (*b*) we show the measured reflectivities of both compounds and in figures 5(*a*) and (*b*) the fitted dielectric functions at 300 and 15 K.

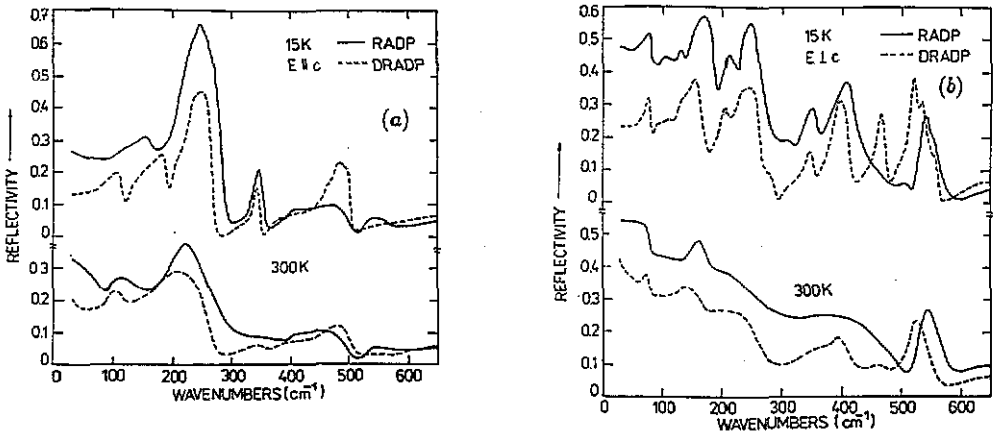

Figure 4. FIR reflectivity of DRADP compared to RADP at 300 and 15 K. (*a*) $E \parallel c$ polarization, (*b*) $E \perp c$ polarization.

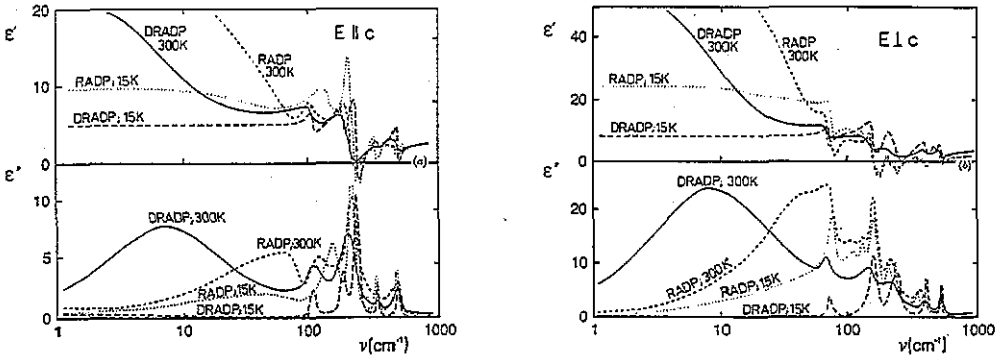

Figure 5. Broad-frequency dielectric spectra of DRADP compared to RADP at 300 and 15 K. (*a*) $E \parallel c$ polarization, (*b*) $E \perp c$ polarization.

The most striking difference between both compounds is the huge isotopic shift of the soft-mode frequency at high temperatures and the background absorption at low temperatures present in RADP but not in DRADP. Let us, however, postpone the discussion of these important effects to the second part of this section and begin with the assignment of vibrational modes.

Our suggestion, which is based on the results of factor group analysis, comparison with RADP spectra (Petzelt *et al* 1991), assignment of Raman modes in RADP (Courtens and Vogt 1985) and general discussion of IR spectra in the KDP-type family (Simon 1992, Vaezzadeh *et al* 1992), is shown in table 1 with the corresponding mode parameters from our fit. Comparison of the corresponding mode frequencies in protonated and deuterated samples shows the strongest isotopic shift for the for the Rb–PO_4 translations and for the E-symmetry $\nu_4(PO_4)$ internal vibration. This is in accordance with the well known fact (Simon 1992) that these two modes are strongly coupled to proton modes. Partly due to their much lower frequency, the interaction with deuteron modes is much weaker, which is evident also from strongly reduced damping of PO_4 internal modes in the case of DRADP.

Similar effects are known from the comparison of pure KDP and DKDP samples (Simon 1992, Bréhat and Wyncke 1988).

Comparing table 1 with the similar table in our previous paper (Kamba *et al* 1992), it is seen that we have made a few minor changes in the assignment. The B_2 mode at 127 cm^{-1} in RADP is now assigned to Rb–PO_4 translation but at low temperatures a PO_4 libration presumably appears in the same spectral range, so that unlike in DRADP these two modes are not well resolved. In the case of DRADP, the libration mode L(PO_4), which is clearly seen in the reflectivity only at low temperatures, lies apparently between the split Rb–PO_4 and ND_4–PO_4 translations, but the modes are strongly coupled. Its clear appearance is further evidence for the local symmetry lowering (clusters) in our glasses below about $T_f \simeq 120$ K, since it is forbidden in the B_2-symmetry spectra of the paraelectric structure (Courtens and Vogt 1985).

Let us briefly comment on this temperature range around 120 K, which shows up also in several other experiments, e.g. in the saturation of the correlation length in diffuse neutron and x-ray scattering (Grimm 1989, Cowley *et al* 1986) or in ^{87}Rb NMR relaxation experiments (Korner 1992). It is probably connected with the freezing of ammonia deuterons (Blinc *et al* 1986a, b), which may create nuclei for a quasi-static cluster formation. Let us stress that it is by no means a sharp, well defined temperature. Within the framework of existing theories (Pirc *et al* 1987, 1991) it corresponds to the region where random interactions begin to dominate over random fields. Let us call it therefore the frustration temperature T_f. It is definitely higher than the nominal glass temperature T_g in the absence of random fields ($\sim$ 90 K) or the de Almeida–Thouless temperature T_{AT} ($\sim$ 50 K) where the ergodicity of the system is broken (Pirc *et al* 1991).

The second change in our assignment concerns the weaker B_2 and E modes near 340 cm^{-1} in both compounds, which are now assigned to $\nu_2(PO_4)$ internal vibration. The previous assignment as NH_4 libration is incompatible with the fact that a similar mode does not appear in pure ADP (Simon 1990) but appears in RDP and DKDP (Simon 1992). Consequently, the highest-frequency B_2 mode in table 1 is assigned to $\nu_4(PO_4)$ internal vibrations in agreement with the assignment of Simon (1992). In E spectra the assignment of $\nu_2(PO_4)$ and $\nu_4(PO_4)$ modes was done using the IR strength argument: ν_4 modes are stronger because, unlike ν_2 modes, they are IR active in the free PO_4 molecules. The appearance of two ν_2 modes, according to the selection rules (Simon 1992), is specific for the antiferroelectric phase.

Now let us come back to the discussion of two main differences between DRADP and RADP samples. The effect of background absorption has already been discussed in our previous papers (Petzelt *et al* 1991, Kamba *et al* 1992), where we suggested that the background absorption is connected with disorder-induced breaking of the quasi-momentum-conservation selection rule. In the case when in the structure clear clusters of average diameter b freeze in (i.e. below T_f), one can expect mainly activation of phonons with the wavevector $2\pi/b$. No essential differences in this effect would be expected for DRADP samples as approximately the same type of cluster develops in them below $T \simeq 120$ K (Cowley *et al* 1986).

In DRADP the background absorption is drastically reduced. Direct transmission measurements in the 15–100 cm^{-1} range have shown that above $\sim$30 cm^{-1} all the absorption at low temperatures can be accounted for by wings of damped oscillators describing the one-phonon absorption. The loss values at 15 K are $\epsilon_a''(30\ cm^{-1}) \simeq 0.08$ and $\epsilon_c''(30\ cm^{-1}) \simeq 0.03$. The analogous values for RADP are $\epsilon_a''(30\ cm^{-1}) \simeq 6$ and $\epsilon_c''(30\ cm^{-1}) \simeq 2$ (Petzelt *et al* 1991).

The experimental fact that a large difference is found between RADP and DRADP

Table 1. Polar phonon parameters in DRADP as compared with those of RADP.

DRADP						RADP						
ν (cm^{-1})		Γ (cm^{-1})		$\Delta\epsilon$		ν (cm^{-1})		Γ (cm^{-1})		$\Delta\epsilon$		
15 K	300 K	15 K	300 K	15 K	300 K	15 K	300 K	15 K	300 K	15 K	300 K	Tentative assignment[a]
B_2 modes ($E \parallel c$)												
110	113	10	38	0.25	0.9	157	127	35	60	1.3	1.0	T(Rb–PO_4) + L(PO_4)
184	202	15	71	0.35	1.2							
235	214	22	60	1.1	0.9	220	217	17	50	1.7	2.0	T(ND_4–PO_4)
345	345	8	28	0.07	0.05	340	340	20	100	0.2	0.2	ν_2(PO_4)
485	481	24	60	0.23	0.25	470	470	150	250	0.4	0.8	ν_4(PO_4)
						75		180		2.8		Background
E modes ($E \perp c$)												
73	69	7	15	0.4	1.5	78	68	12	15	2.4	1.4	L(PO_4) + T(Rb–PO_4)
105	105	40	80	0.65	1.3	120	—	40	—	1.6	0	
147	143	25	50	1.9	2.2	165	159	22	30	2.5	1.6	
200	185	8	60	0.2	0.2	208	208	16	30	0.3	0.2	T(ND_4–PO_4)
230	218	33	90	1.1	1.9	238	238	14	80	0.5	0.7	
347	347	2	17	0.02	0.08	348	349	20	40	0.2	0.04	ν_2(PO_4)
390	392	22	45	0.4	0.38	397	405	21	140	0.2	1.2	ν_4(PO_4)
460	463	11	25	0.12	0.03	—	—	—	—	—	—	ν_2(PO_4)
518	520	25	30	0.25	0.25	540	544	16	25	0.1	0.2	ν_4(PO_4)
						165		300		15		Background

[a] L, libration; T, translation; ν_i, internal modes.

concerning this background absorption speaks against the above-mentioned interpretation in the case of RADP. Another possible explanation is that the distribution of energy barriers between the minima in the proton double-well potentials is much broader than in the case of deuteron ones, especially on the low-energy side. In fact, such a model was successfully used for fitting the low-temperature ($T \leqslant 115$ K) Raman central peak in RADP by Courtens and Vogt (1986). These authors used for the fit a constant distribution of Debye relaxations from short attempt time corresponding to frequency $\nu_\infty = 120\ \mathrm{cm}^{-1}$ (3.6×10^{12} Hz) (Rb–PO_4 translations) up to the cut-off time obeying the Vogel–Fulcher law. Also in fitting the dielectric data (Courtens 1984, 1986, Brückner *et al* 1988) only the high-energy barrier height cut-off could have been established for measuring frequencies up to 10^{10} Hz. This is a consequence of the fact that for any temperature the dielectric losses in RADP are only increasing or constant functions of frequency up to the FIR range (with a broad high-frequency plateau at low temperatures) (Petzelt *et al* 1991, Brückner *et al* 1988). This dielectric behaviour sharply contrasts with that in DRADP where clear maxima in $\epsilon''(\nu)$ spectra were found for all temperatures (Courtens 1986, He *et al* 1990, He 1991, figure 3 of this paper). Therefore the energy barrier distribution in DRADP has a clear low-energy cut-off described well by the temperature-independent Gaussian distribution with mean energy $E_0 \simeq 390$ K and variance $\sigma \simeq 95$ K in the Vogel–Fulcher law for the relaxation times (He *et al* 1990).

This striking difference between RADP and DRADP has to our knowledge not yet been discussed microscopically. It has its manifestation also in thermal properties (Berret *et al* 1991), which point to a much more pronounced glassy behaviour of RADP than DRADP.

The non-Gaussian energy barrier distribution at the low-energy end in the case of RADP might be only an apparent effect caused by quantum tunnelling of protons between both potential minima. The distribution of O–H···O hydrogen bond length caused by the disorder introduced by NH_4 groups leads to a distribution of distances between the potential minima. This may give a distribution of proton tunnelling frequencies broader than the distribution of classical hopping frequencies of deuterons in a comparable barrier distribution (Matsushita and Matsubara 1982). Moreover, both mechanisms may combine—the classical thermally (or Vogel–Fulcher) activated hopping at the low-frequency absorption end and quantum tunnelling (not so strongly temperature dependent) dominating at higher frequencies.

The huge isotopic shift of the soft-mode frequency is well known from pure compounds (Simon 1992) and in our glass system was also observed in the low-frequency dielectric spectra (Courtens 1986, He *et al* 1990, He 1991) and in NMR spectra (Slak *et al* 1984, Blinc *et al* 1986a, b). We shall come back to this point more quantitatively at the end of our discussion.

Let us now discuss the connection between our high-frequency and existing low-frequency dielectric data. Up to now a global approach was used for discussion of the proton dynamics in RADP-35 (Courtens and Vogt 1986) including the FIR data (Simon and Gervais 1992, Simon 1992). It is based on plotting the lower cut-off frequency characterizing the proton dynamics as a function of temperature and demonstrating the validity of the Vogel–Fulcher law for it. It should be remembered that the treated proton dynamics concerns only the uniform proton motion in the Brillouin-zone centre owing to the experimental techniques used (dielectric and light scattering spectroscopy). In this case one can directly determine the complex response function of the proton system as the dielectric or light scattering susceptibility whose imaginary part is proportional to the spectral density of uniform proton motion. However, comparison with other techniques that probe the local proton dynamics, i.e. the integral of low-frequency proton motion over the whole Brillouin zone, like incoherent neutron scattering (Grimm *et al* 1989) or NMR (Slak *et al* 1984)

shows that—at least below T_f—there are no essential differences between the low-frequency uniform and local proton dynamics.

The characteristic lower cut-off frequency used for the Vogel–Fulcher fit was uniquely defined only under the assumption that the spectral distribution of relaxation times in the proton dynamics is much broader than the response of one Debye relaxation. This is justified at low temperatures, well below T_f. Above T_f it is known from high-frequency probes (Petzelt *et al* 1991, Courtens and Vogt 1986) that the proton dynamics is essentially monodispersive, i.e. it can be described by one Debye relaxation, and the determination of the cut-off frequency becomes somewhat ambiguous.

Another approach to fit the dielectric spectra and demonstrate the validity of the Vogel–Fulcher dependence was used by He *et al* (1990) and He (1991). These authors have shown that the complex dielectric spectrum in the 10^3–10^9 Hz range below $\sim$ 100 K can be well fitted with a distribution of Debye relaxations assigned to proton or deuteron hopping over energy barriers with temperature-independent Gaussian distribution of heights. In this model the natural characteristic frequency is the hopping frequency over the mean barrier, which corresponds to the maximum in the $\epsilon''(\nu)$ spectrum. He *et al* (1990) have shown that this frequency also follows the Vogel–Fulcher dependence even if the parameters are slightly different from those in the fit by Courtens and Vogt (1986). This must be expected since Courtens' characteristic frequency is orders of magnitude lower at low temperatures (about 10^2 Hz at 20 K, whereas it is about 10^8 Hz in the fit by He). This difference, however, reduces on increasing the temperature, and in the high-frequency and high-temperature limit the attempt frequency is not expected to differ.

It is not clear *a priori* which approach to demonstrate the Vogel–Fulcher dependence is the better one. In fact, both give good results with practically the same T_{VF}. However, the latter approach is not limited to a broad distribution of relaxation times and can be naturally used also in the FIR range above T_f—the characteristic frequency is then just the Debye relaxation frequency. Actually, we were able to fit successfully our data on RADP-50 for both polarizations together with the data of He with a Vogel–Fulcher law with the following parameters common to both polarizations: $T_{VF} = 10.5$ K, $E_0 = 95$ K and $\nu_\infty = 60$ cm^{-1} (1.8×10^{12} Hz). The T_{VF} and E_0 parameters are somewhat correlated: increase in T_{VF} by 1 K combined with a decrease in E_0 by 15 K still yields an acceptable fit. However, a fit with an Arrhenius law is completely unacceptable because of the low value of ν_∞ fixed by our high-frequency data. Comparison with the fitted parameters of He shows a good agreement with much higher accuracy of the ν_∞ value in our case.

Our value $\nu_\infty = 60$ cm^{-1} is, however, only half of the value obtained from the fit by Courtens and Vogt. This is caused by a smaller slope in our ν_R versus $1/(T - T_{VF})$ plot compared to that in Courtens' plot, owing to different definition of ν_R, as already discussed. Our value of ν_∞ directly corresponds to the asymptotic high-temperature value of ν_R. Taking this frequency we neglect the coupling of the proton mode with higher-frequency lattice and internal PO_4 modes (Simon 1992). Another approach (presumably a more correct one) would be to decouple the proton mode from other modes and use the bare uncoupled-mode frequency for the Vogel–Fulcher plot. In fact, the decoupling has been partially performed by Courtens and Vogt (1985). It shows that the bare proton frequency really increases appreciably compared to the observed coupled one and at high temperatures reaches 120 cm^{-1}. With such a high value of ν_∞, a slightly lower T_{VF} would result, in complete agreement with the fit by Courtens and Vogt (1986).

The fit of dielectric spectra of RADP suffers from one drawback already mentioned: the maxima in $\epsilon''(\nu)$ spectra are not clearly seen at any temperature so that the fitting parameters are extracted only from the low-frequency parts of the loss peaks. This is

mostly true also for our FIR data, especially in the case of the $E \perp c$ polarization owing to the background absorption already discussed. It may somehow question the reliability of the fitting procedure. This drawback is removed in the case of DRADP where well developed loss peaks symmetrical in $\lg(\nu)$ around ν_R have been observed and fitted (Xhonneux *et al* 1988, He 1991).

In figures 6(*a*) and (*b*) we show that our data on DRADP for ν_R together with data from He can be well fitted with a Vogel–Fulcher law. Our fitting parameters agree with those of He except for ν_∞, which again can be fitted much more accurately from our data. Let us stress that, like the data of He, our data on ν_R are within the accuracy limit isotropic, with the following Vogel–Fulcher parameters: $T_{VF} = 34 \pm 3$ K, $E_0 = 410 \pm 5$ K, $\nu_\infty = 39 \pm 3$ cm^{-1} ($(1.17 \pm 0.09) \times 10^{12}$ Hz). The only appreciable anisotropy in our low-frequency spectra concerns the dielectric strength of the dispersion and consequently the extrapolated static permittivity value ϵ_0. In our case of $x = 0.5$, $\epsilon_0(E \parallel c) < \epsilon_0(E \perp c)$, which is known also from other dielectric measurements and naturally depends on the ND_4 concentration x (for $x < 0.3$ the reverse situation is expected—see He (1991)). Let us note that the anisotropy is temperature dependent and the ratio $\epsilon_0(E \perp c)/\epsilon_0(E \parallel c)$ decreases somewhat with decreasing temperature.

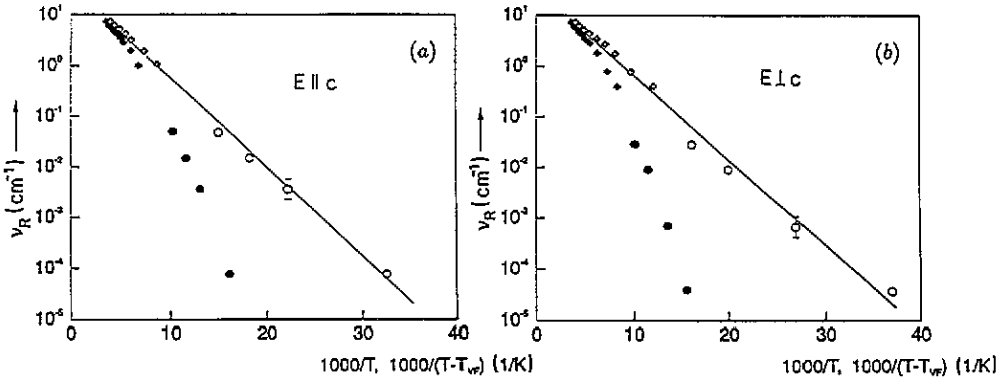

Figure 6. Temperature dependence of the low frequency $\epsilon''(\nu)$ maxima (crosses) combined with lower-frequency data from He (1991). The two plots demonstrate the validity of the Vogel–Fulcher law: open symbols correspond to the Vogel–Fulcher plot and full symbols to the Arrhenius plot. (*a*) $E \parallel c$ polarization; full line represents the Vogel–Fulcher law with $T_{VF} = 32$ K, $E_0 = 410$ K, $\nu_\infty = 37$ cm^{-1}. (*b*) $E \perp c$ polarization; the full line represents the Vogel–Fulcher law with $T_{VF} = 37$ K, $E_0 = 410$ K, $\nu_\infty = 40$ cm^{-1}.

In figure 7 we plot our deuteron mode frequency on a linear frequency scale. The striking feature is that, within the limits of experimental accuracy, besides the Vogel–Fulcher fit (full curve), the data can be nicely fitted also with an Arrhenius law ($E_0 = 500$ K, $\nu_\infty = 39$ cm^{-1}, chain curve) or even with a classical softening law $\nu_R = A(T - T_c)$ ($A = 0.043$ cm^{-1} K^{-1}, $T_c = 120$ K, broken curve).

In this connection it is important to note that exactly the same relaxation frequency and softening were obtained from inelastic neutron scattering on DRADP-62 near the wavevector $q_m = 0.35a^*$ where the maximum of quasielastic diffuse scattering was observed (Grimm and Martinez 1986, Xhonneux *et al* 1988). This shows that above T_f the deuteron dynamics is practically q independent and its collective nature is only weak. The same conclusion can be drawn also for the dynamics below T_f, where as in protonated systems the deuteron

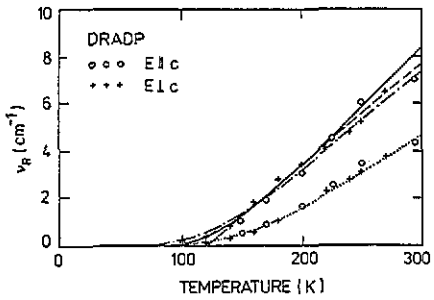

Figure 7. Soft deuteron mode frequency in DRADP above T_g for both polarizations (upper data set). The broken curve corresponds to the classical softening law $\nu_R = A(T - T_c)$ where $A = 0.043$ cm^{-1} K^{-1} and $T_c = 120$ K. The full curve corresponds to the Vogel–Fulcher law $\nu_R = \nu_\infty \exp[-E_0/(T - T_{VF})]$ with $\nu_\infty = 39$ cm^{-1}, $E_0 = 410$ K and $T_{VF} = 34$ K. The chain curve corresponds to the Arrhenius law $\nu_R = \nu_\infty \exp(-E_0/T)$ with $\nu_\infty = 39$ cm^{-1} and $E_0 = 500$ K. The lower plot corresponds to the calculated single-particle hopping frequency for both polarizations. The dotted curve corresponds to an Arrhenius fit with $\nu_\infty = 39$ cm^{-1} and $E_0 = 640$ K.

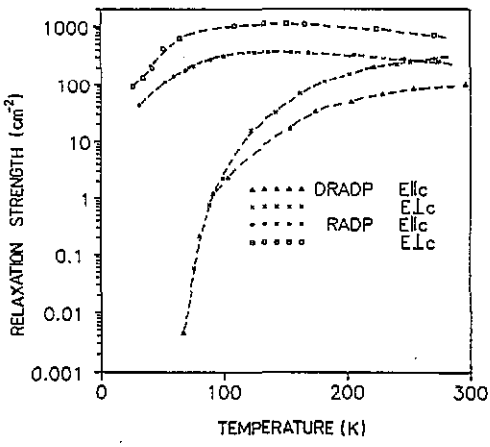

Figure 8. Temperature dependence of the relaxation strength $\Delta\epsilon\nu_R$ of the deuteron mode as compared with that of the proton mode. Low-temperature data for DRADP are calculated from data of He (1991); data on RADP are taken from Petzelt *et al* (1991).

dynamics deduced from dielectric data is compatible with the total dynamics from NMR data (Korner 1992). This means that the softening of deuterons (protons) is prevailingly due to their individual freezing. Therefore the Arrhenius or Vogel–Fulcher softening law is more appropriate for fitting the ν_R data for $T > T_f$ than the classical linear law.

In figure 8 we plot the relaxation strength $\Delta\epsilon\nu_R$ ($\Delta\epsilon$ is the contribution of the dielectric relaxation to the static permittivity) as a function of temperature for both polarizations and compare it with a similar plot for RADP (Petzelt *et al* 1991). The results from lower-frequency data of He are also included in the case of DRADP. Notice the tremendous decrease of strength on lowering the temperature. This quantity is usually considered to be roughly temperature independent above ferroelectric and antiferroelectric transitions because the Curie–Weiss increase in $\Delta\epsilon$ is compensated by softening of ν_R. Below classical order–disorder ferroelectric transitions this quantity decreases and the dynamical Ising model in the mean-field approximation yields (Blinc and Žekš 1974)

$$\Delta\epsilon\nu_R = (C\nu_0/T)(1 - 4\langle s^z\rangle^2) \tag{2}$$

where C is the Curie constant, ν_0 is the single-particle relaxation frequency (obeying the Arrhenius law) and the time-average spin value $\langle s^z\rangle$ represents the spontaneous order parameter for the phase transition. It is seen that this quantity vanishes when the order parameter saturates ($\langle s^z\rangle \to 1/2$). (This is remarkably different behaviour from that in displacive transitions where the analogous quantity—soft oscillator strength—remains finite down to 0 K. Therefore this quantity can be used for distinguishing between displacive and order–disorder transitions in the case of overdamped soft modes.)

In the case of dipolar glasses equation (2) can still be used approximately just by substituting $\langle s^z\rangle^2$ by the Edwards–Anderson order parameter $q \equiv 4(\langle s^z\rangle^2)_{AV}$ (Tadic *et al* 1989). Heuristic argumentation is the following. Equation (2) describes the fact that those particles which become frozen (ordered) do not hop any more, i.e. do not absorb at low frequencies, and, therefore, do not contribute to the permittivity and relaxation strength. For it to be valid it is not necessary to have a macroscopic ordering but local microscopic ordering or even individual freezing is sufficient.

In our case of DRADP-50 the relaxation strength decreases to zero practically by the same law as ν_R or, in other words, $\Delta\epsilon$ is only weakly temperature dependent (above $\simeq$ 200 K it can be approximately fitted with a Curie–Weiss law with $T_c \simeq -200$ K for both polarizations). This indicates a saturation of the Edwards–Anderson parameter at $T = T_{VF}$. It should be remembered, however, that close to T_{VF} the ergodicity in a real finite observation time is broken, so that the discussed laws are no longer valid. Particularly one can expect non-zero (but time- and path-dependent) absorption even at temperatures $T \leqslant T_{VF}$.

Figure 8 shows that unlike in RADP the relaxation strength in DRADP decreases even from room temperature. This is caused mainly by softening of ν_0 but indicates also the possibility of non-zero $q(T)$ due to random field effects. Taking the $q(T)$ values as determined from NMR experiments (Blinc *et al* 1989) and using the approximate values for the Curie constant from the high-temperature ($T > 200$ K) behaviour of $\Delta\epsilon$ ($C(E \parallel c) = 7350$ K^{-1}, $C(E \perp c) = 25\,000$ K^{-1}), we can calculate the single-particle hopping frequency. The result is plotted in figure 7 (lower-frequency plot) together with a fit with the Arrhenius law $\nu_0 = \nu_\infty \exp(-E_0/T)$ with $\nu_\infty = 39$ cm^{-1} and $E_0 = 640$ K. The same value of ν_∞ as in the case of the collective relaxation frequency ν_R is, of course, expected. The value of the activation energy E_0 is, however, determined mainly by the value of C, which is not very accurate.

From the above discussion it becomes clear that the softening of the deuteron mode above T_f is essentially due to slowing down of the single-particle hopping. Such a pronounced slowing down in our limited temperature interval is caused by unusually low attempt frequency ν_∞ ($\tau_\infty = 1.36 \times 10^{-13}$ s) and energy barrier height E_0 and has, to the authors' knowledge, not yet been observed near other order–disorder transitions. The low ν_∞ and E_0 values, which are probably not limited to mixtures in the glass range but are expected also in pure RbD_2PO_4 (DRDP) and $(ND_4)D_2PO_4$ (DADP) crystals, may be caused by coupling of the deuteron hopping motion to polar phonon modes, which should strongly hybridize the modes in analogy to the KDP–DKDP system (Simon 1992). The large isotopic effect on some of the polar phonon modes in RADP and DRADP (see above) points to the importance of this coupling but does not simply allow one to estimate its strength. Hence, our low ν_∞ and E_0 parameters concern rather the mixed deuteron–lattice hopping than hopping of bare deuterons.

It is interesting to note that the proton softening process in RADP is rather different. The softening is much less pronounced (Petzelt *et al* 1991) and the relaxation strength begins to decrease only below $T_f \simeq 100$ K. This picture is not compatible with the classical Ising model and calls for consideration of proton tunnelling.

Up till now we have tried to describe the deuteron dynamics in a unified way for the whole temperature region below $\sim$ 300 K even if the dielectric dispersion becomes polydispersive below $T_f \simeq 120$ K, which supports the structural picture that some quasi-static inhomogeneity due to increasing correlations develops in the system (Cowley *et al* 1986, Grimm 1989). The unified description does not sharply distinguish between the dynamics of deuterons inside the small ($\sim$ 20 Å) clusters and in regions between them. In

this picture the acid deuterons inside the clusters still jump, but in an asymmetric double-well potential biased by the random field (produced e.g. by frozen ammonia groups). There is no qualitative difference between the deuteron dynamics inside the clusters and in regions between them, or, in other words, no appearance of pronounced clusters with well defined cluster walls.

An alternative picture for the acid deuteron dynamics below T_f would be creation of well defined ordered clusters in which the deuterons are essentially frozen, separated by active regions where the deuterons still jump. This picture is supported by molecular-dynamics calculations (Parlinski and Grimm 1988) and is more probable at sufficiently low temperatures. Structurally, the ordered clusters may consist of regions where the ice rules are satisfied (Matsushita and Fuchizaki 1987) separated by regions with high concentration of Takagi defects (HPO_4^{2-} and/or H_3PO_4 groups) where the deuterons are still jumping, causing the local diffusion of these defects. This motion has already been assigned to the broad dielectric dispersion in RADP below T_f (Schmidt 1988a, b).

According to this alternative picture, the monodispersive deuteron mode that is assigned to all acid deuterons above T_f should gradually disappear below T_f and transfer into a weaker polydispersive mode assigned to deuteron hopping in the regions between quasi-static ordered clusters. In the vicinity of T_f one could expect a more complex dielectric dispersion consisting of both types of contribution—a higher-frequency dispersion from the hopping inside the clusters and a lower-frequency one predominantly from the diffusion of Takagi defects between the clusters. Unfortunately, the available dielectric data do not allow one to distinguish between these pictures. To do so would require careful dielectric measurements around 120 K in the still missing 1–100 GHz range or, at least, in the more limited 3–30 GHz range.

5. Conclusion

From the detailed comparison of DRADP-50 and RADP-50 high-frequency dielectric response we can conclude the following:

Proton motion seems to be more strongly coupled to phonons than deuteron motion. This leads to strong isotopic shift of lattice translation T(Rb–PO_4) mode frequencies and to strong reduction of internal $\nu_4(PO_4)$ and $\nu_2(PO_4)$ mode dampings on deuteration.

The low-frequency proton mode shows a large isotopic shift down on deuteration. The averaged characteristic frequency in both cases exhibits a Vogel–Fulcher-type behaviour in a broad temperature range with the following parameters: $T_{VF}(H) = 10.5$ K, $T_{VF}(D) = 34$ K, $E_0(H) = 95$ K, $E_0(D) = 410$ K, $\nu_\infty(H) = 1.8 \times 10^{12}$ Hz, $\nu_\infty(D) = 1.17 \times 10^{12}$ Hz.

Within the accuracy limits of our experiment above ~ 120 K this softening can also be described by an Arrhenius law or by classical slowing down in a compound with averaged structure with a long-range phase transition. However, collective effects in the deuteron dynamics are only of minor importance.

Several qualitative differences between proton and deuteron dynamics indicate the presence of broad-frequency tunnelling in the protonated compound:

(i) absence of clear $\epsilon''(\nu)$ maxima in the case of RADP at any temperature—the losses persist up to phonon frequencies;

(ii) even in the range of FIR phonon frequencies the proton motion gives rise to broad background absorption, which is coupled especially to ν_2 and $\nu_4(PO_4)$ internal modes, dramatically increasing their damping;

(iii) at higher temperatures above T_f the tunnelling probably prevents local freezing of protons, which is indicated by the high relaxation strength of the proton mode and its different temperature dependence than in the case of the deuteron mode.

Acknowledgments

The authors would like to thank M Ehrensperger for crystal growth. Helpful discussions with N Korner, O Hudak and P Simon and critical reading of the manuscript by I Gregora are acknowledged. The work was supported by the Czech Grant Agency (No. 11081) and by the Swiss National Science Foundation.

References

Arend H, Perret R, Wüest H and Kerkoč P 1986 *J. Cryst. Growth* **74** 321
Berret J-F, Meissner M, Watson K S, Pohl R O and Courtens E 1991 *Phys. Rev. Lett.* **67** 93
Blinc R, Ailion D C, Günther B and Žumer S 1986a *Phys. Rev. Lett.* **57** 2826
Blinc R, Dolinšek J, Pirc R, Tadič B, Zalar B, Kind R and Liechti O 1989 *Phys. Rev. Lett.* **63** 2248
Blinc R, Günther B and Ailion D C 1986b *Phys. Scr.* T **13** 205
Blinc R and Žekš B 1974 *Soft Modes in Ferroelectrics and Antiferroelectrics* (Amsterdam: North-Holland) p 152
Bréhat F and Wyncke B 1988 *J. Phys. C: Solid State Phys.* **21** 4853
Brückner H J, Courtens E and Unruh H-G 1988 *Z. Phys.* B **73** 337
Courtens E 1984 *Phys. Rev. Lett.* **52** 69
—— 1986 *Phys. Rev.* B **33** 2975
—— 1987 *Ferroelectrics* **72** 229
Courtens E and Vogt H 1985 *J. Chim. Phys.* **82** 317
—— 1986 *Z. Phys.* B **62** 143
Cowley R A, Ryan T W and Courtens E 1986 *Z. Phys.* B **65** 181
Grimm H 1989 *Dynamics of Disordered Materials (Springer Proc. Phys. 37)* ed D Richter *et al* (Berlin: Springer) p 274
Grimm H, Courtens E, Dorner B and Monkenbusch M 1989 *Physica* B **156–157** 192
Grimm H and Martinez J 1986 *Z. Phys.* B **64** 13
He P 1991 *J. Phys. Soc. Japan* **60** 313
He P, Deguchi K, Hirokane M and Nakamura E 1990 *J. Phys. Soc. Japan* **59** 1835
Höchli U T, Knorr K and Loidl A 1990 *Adv. Phys.* **39** 405
Kamba S, Petzelt J, Sinitski A V, Pimenov A G, Volkov A A and Kozlov G V 1992 *Ferroelectrics* **127** 263
Kind R, Mohr M, Schiemann G and Liechti O 1990 *Ferroelectrics* **106** 125
Korner N 1992 *PhD Thesis* ETH, Zürich
Matsushita E and Fuchizaki K 1987 *Japan. J. Appl. Phys.* **26** S-3 793
Matsushita E and Matsubara T 1982 *Prog. Theor. Phys.* **67** 1
Parlinski K and Grimm H 1988 *Phys. Rev.* B **37** 1925
Petzelt J, Železný V, Kamba S, Sinitski A V, Lebedev S P, Volkov A A, Kozlov G V and Schmidt V H 1991 *J. Phys.: Condens. Matter* **3** 2021
Pirc R, Tadic B and Blinc R 1987 *Phys. Rev.* B **36** 8607
Pirc R, Tadic B, Blinc R and Kind R 1991 *Phys. Rev.* B **43** 2501
Schmidt V H 1988a *Ferroelectrics* **78** 207
—— 1988b *J. Mol. Struct.* **177** 257
Simon P 1990 *Ferroelectrics* **107** 133
—— 1992 *Ferroelectrics* **135** 169
Simon P and Gervais F 1992 *Ferroelectrics* **125** 461
Slak J, Kind R, Blinc R, Courtens E and Žumer S 1984 *Phys. Rev.* B **30** 85
Tadic B, Pirc R and Blinc R 1989 *Z. Phys.* B **74** 249
Vaezzadeh M, Wyncke B and Bréhat F 1992 *J. Phys.: Condens. Matter* **4** 7401
Volkov A A, Goncharov Yu G, Kozlov G V, Lebedev S P and Prokhorov A M 1985 *Infrared Phys.* **25** 369
Xhonneux P, Courtens E and Grimm H 1988 *Phys. Rev.* B **38** 9331